Journal of Systems Engineering and Electronics
Vol. 34, No. 3, June 2023, pp.766 – 774

Distributed fault diagnosis observer for multi-agent system against actuator and sensor faults

YE Zhengyu, JIANG Bin*, CHENG Yuehua, YU Ziquan, and YANG Yang
College of Automation Engineering, Nanjing University of Aeronautics and Astronautics, Nanjing 210016, China

Abstract: Component failures can cause multi-agent system (MAS) performance degradation and even disasters, which provokes the demand of the fault diagnosis method. A distributed sliding mode observer-based fault diagnosis method for MAS is developed in presence of actuator and sensor faults. Firstly, the actuator and sensor faults are extended to the system state, and the system is transformed into a descriptor system form. Then, a sliding mode-based distributed unknown input observer is proposed to estimate the extended state. Furthermore, adaptive laws are introduced to adjust the observer parameters. Finally, the effectiveness of the proposed method is demonstrated with numerical simulations.

Keywords: multi-agent system (MAS), sensor fault, actuator fault, unknown input observer, sliding mode, fault diagnosis.

DOI: 10.23919/JSEE.2023.000047

1. Introduction

In the last decade, multi-agent systems (MAS) have attracted vast amounts of the attention. In comparison with single dynamics system, the merits of MAS include low cost, high reliability, and good scalability [1]. MAS such as unmanned aerial vehicles (UAV), unmanned ground vehicles (UGV), multi-robot systems, and UAV-UGV cooperative teams have been devoted into applications and make huge profits [2−8]. The MAS is more likely to encounter faults as the amount of agents increases. However, the distributed fault diagnosis problem receives few concerns comparing with the distributed control problem.

The existing distributed fault diagnosis researches mainly address the actuator fault problem [9−12]. It is because the actuator fault has no impact on the measurement of the system state, which eases the fault diagnosis method design for MAS [13]. Different from the actuator fault, the sensor fault disturbs the measurement of the system state [14−16]. The fault detection is not affected by sensor fault, while the fault estimation is challenging without a reliable measurement [17]. There are few studies carried out on the sensor fault diagnosis problem in comparison with actuator fault, in which only minority of them aims at MAS [18−21]. Among the studies on sensor fault diagnosis, the descriptor system approach is popular owning to its mature and plentiful analysis methods on singular system, which facilitates the study by extending the sensor fault into the system states [22−28]. However, these works focus on the single dynamics system.

To our best knowledge, there are only handful studies addressing the distributed sensor fault diagnosis problem of MAS [29−33]. The existing works carry out the study by transforming the system into a descriptor form, for which the observer is then designed to estimate the extended system states. By introducing the distributed feedback items in the observer, the fault diagnosis is performed based on information from neighboring agents. The sensor fault estimation is finally extracted from the extended states estimation. Nevertheless, the upper bounds of the faults which are assumed to be known in these works are usually unavailable in practice. The observation effectiveness relies on the proper setting of the values of the fault bounds, which motivates the study of this paper.

This paper develops an adaptive sliding mode-based distributed fault diagnosis method for MAS with actuator and sensor faults. The contribution of this paper primarily lies in the following features:

(i) Different from [18−21] of which the subject is single dynamic system, this paper studies the distributed fault diagnosis of MAS. A distributed feedback term is introduced to guarantee the stability of the overall estimation error dynamics.

(ii) Different from [9−12] which address the dis-

Manuscript received March 02, 2022.
*Corresponding author.
This work was supported by the National Natural Science Foundation of China (62020106003;62003162), 111 project (B20007), the Natural Science Foundation of Jiangsu Province of China (BK20200416), and the China Postdoctoral Science Foundation (2020TQ0151; 2020M681590).

tributed actuator fault diagnosis, the actuator and sensor faults are considered simultaneously in this work. To avoid the sensor fault disturbing the observation, the MAS is transformed into a descriptor system form.

(iii) Comparing with [29,30,32,33], an adaptive law is introduced to update the sliding mode feedback term which reduces the requirements on the priori knowledge of the MAS.

The structure of this paper is organized as follows. Section 2 introduces the system and some fundamental knowledge. Section 3 is devoted to the main results, i.e., the system transformation, the distributed observer design, and the stability analysis. Section 4 demonstrates the effectiveness of the proposed method.

Notations: In this paper, the definitions of some symbols and operations are given as follows. For a vector $\boldsymbol{v} = [v_1, v_2, \cdots, v_n]^{\mathrm{T}} \in \mathbf{R}^n$, $\|\boldsymbol{v}\|$ represents its norm value. $\operatorname{sign}(\boldsymbol{v}) = \dfrac{\boldsymbol{v}}{\|\boldsymbol{v}\|}$ is the signum function. $\boldsymbol{I}_n$ and $\boldsymbol{0}_{p\times q}$ represent an $n\times n$ identity matrix and a $p\times q$ matrix with 0 as all its elements, respectively. $\otimes$ is the Kronecker product. $\boldsymbol{M}^{\mathrm{T}}$ is the transpose of matrix $\boldsymbol{M}$, and $\boldsymbol{M}^{-\mathrm{T}}$ is the inverse of $\boldsymbol{M}^{\mathrm{T}}$ if $\boldsymbol{M}$ is invertible.

2. Preliminaries and problem formulation

2.1 Graph theory

Algebraic graph theory is introduced to describe the communication relationships among the MAS. A directed graph $\mathcal{G} = (\upsilon, \varepsilon, \mathcal{A})$ consists of a vertices set $\upsilon = \{\upsilon_1, \upsilon_2, \cdots, \upsilon_l\}$, an edge set $\varepsilon \subseteq \upsilon\times\upsilon$ in which $\varepsilon_{ij} \in \varepsilon$ if there is a communication link from vertex i to vertex j, and $\mathcal{A} = [a_{ij}] \in \mathbf{R}^{l\times l}$ is the adjacency matrix in which $a_{ij} > 0$ if $\varepsilon_{ij} \in \varepsilon$, $a_{ij} = 0$ if $\varepsilon_{ij} \notin \varepsilon$ or $i = j$. Denote $\mathcal{D} = \operatorname{diag}(d_1, d_2, \cdots, d_l)$ as the degree matrix of graph $\mathcal{G}$, in which $d_i = \sum_{i=1}^{N} a_{ij}$ is the incoming communication weights sum of vertex υ_i. The Laplacian matrix of graph $\mathcal{G}$ is denoted by $\mathcal{L} = \mathcal{D} - \mathcal{A}$.

Lemma 1 [34] Denote $\mathcal{A}' = \frac{1}{2}(\mathcal{A} + \mathcal{A}^{\mathrm{T}})$ and $\mathcal{L}' = \frac{1}{2}(\mathcal{L} + \mathcal{L}^{\mathrm{T}})$ as the adjacency matrix and Laplacian matrix of a new undirected graph, respectively. If $\mathcal{G}$ is connected, then $\mathcal{G}'$ is also connected. $\mathcal{L}'$ is a symmetric positive semi-definite matrix.

Lemma 2 [35] According to eigenvalue decomposition theory, there exists an orthogonal matrix $\boldsymbol{M}$ that satisfies $\boldsymbol{M}\boldsymbol{M}^{\mathrm{T}} = \boldsymbol{I}$ and $\boldsymbol{M}^{\mathrm{T}}\mathcal{L}'\boldsymbol{M} = \boldsymbol{\Lambda}_2 = \operatorname{diag}(\lambda_1', \lambda_2', \cdots, \lambda_l')$ where $0 = \lambda_1' \leqslant \lambda_2' \leqslant \cdots \leqslant \lambda_l'$.

2.2 Problem formulation

Consider a MAS consists of l agents among which the communication connections are described with a directed graph $\mathcal{G} = (\upsilon, \varepsilon, \mathcal{A})$. The dynamics of agent $i (i = 1, 2, \cdots, l)$ is formulated as

$$\begin{cases} \dot{\boldsymbol{x}}_i(t) = \boldsymbol{A}\boldsymbol{x}_i(t) + \boldsymbol{B}\boldsymbol{u}_i(t) + \boldsymbol{F}_a\boldsymbol{f}_{\mathrm{ai}}(t) \\ \boldsymbol{y}_i(t) = \boldsymbol{C}\boldsymbol{x}_i(t) + \boldsymbol{D}\boldsymbol{u}_i(t) + \boldsymbol{F}_s\boldsymbol{f}_{\mathrm{si}}(t) \end{cases} \tag{1}$$

where $\boldsymbol{x}_i \in \mathbf{R}^n$, $\boldsymbol{y}_i \in \mathbf{R}^m$, and $\boldsymbol{u}_i \in \mathbf{R}^{n_u}$ are the system states, output, and input, respectively. $\boldsymbol{A} \in \mathbf{R}^{n\times n}$, $\boldsymbol{B} \in \mathbf{R}^{n\times n_u}$, $\boldsymbol{C} \in \mathbf{R}^{m\times n}$, and $\boldsymbol{D} \in \mathbf{R}^{m\times n_u}$ are the parametric matrices of the system. $\boldsymbol{f}_{\mathrm{ai}} \in \mathbf{R}^p$ and $\boldsymbol{f}_{\mathrm{si}} \in \mathbf{R}^q$ represent the actuator fault and sensor fault, respectively. $\boldsymbol{F}_a \in \mathbf{R}^{n\times p}$ and $\boldsymbol{F}_s \in \mathbf{R}^{m\times q}$ stand for the parametric matrices of system faults.

Assumption 1 There exist unknown positive constants r_a, $r_{a\delta}$, and r_s such that $\|\boldsymbol{f}_{\mathrm{ai}}(t)\| \leqslant r_a$, $\|\dot{\boldsymbol{f}}_{\mathrm{ai}}(t)\| \leqslant r_{\mathrm{a}\delta\delta}$, and $\|\boldsymbol{f}_{\mathrm{ai}}(t)\| \leqslant r_s$ hold for all $i (i = 1, 2, \cdots, l)$.

Assumption 2 For system (1), the dimensions of actuator fault $\boldsymbol{f}_{\mathrm{ai}}$ and sensor fault $\boldsymbol{f}_{\mathrm{si}}$ satisfy $p + q \leqslant m$.

Assumption 3 System (1) satisfies conditions $\operatorname{rank}(\boldsymbol{F}_a) \geqslant p$ and $\operatorname{rank}(\boldsymbol{F}_s) \geqslant q$.

Remark 1 Since the observer achieves the system states estimation through the system output, the system output has no redundancy if the fault vector can be fully decoupled for all dimensions of the system output. In this case, it is impossible to achieve a reliable state estimation from the system output. Assumption 2 and Assumption 3 set restrictions to the system faults. On the one hand, this avoids the fault decoupling issue. On the other hand, this avoids the problem that the fault parametric matrices being uninvertible such that we cannot gain observation for each dimension of faults.

Throughout this paper, we study the fault diagnosis method for MAS consists of l agents with dynamics (1) in presents with actuator fault $\boldsymbol{f}_{\mathrm{ai}}$ and sensor fault $\boldsymbol{f}_{\mathrm{si}}$.

3. Main results

In this paper, the distributed fault diagnosis is studied on the basis of the descriptor system model. First, we extend the actuator and sensor faults to the system state and rewrite the system (1) into a descriptor system form as

$$\begin{cases} \bar{\boldsymbol{E}}\dot{\bar{\boldsymbol{x}}}_i(t) = \bar{\boldsymbol{A}}\bar{\boldsymbol{x}}_i(t) + \bar{\boldsymbol{B}}\boldsymbol{u}_i(t) + \bar{\boldsymbol{F}}\bar{\boldsymbol{f}}_i(t) \\ \boldsymbol{y}_i(t) = \bar{\boldsymbol{C}}\bar{\boldsymbol{x}}_i(t) + \boldsymbol{D}\boldsymbol{u}_i(t) \end{cases} \tag{2}$$

where $\bar{\boldsymbol{x}}_i = [\boldsymbol{x}_i^{\mathrm{T}}, \boldsymbol{f}_{\mathrm{ai}}^{\mathrm{T}}, \boldsymbol{f}_{\mathrm{si}}^{\mathrm{T}}]^{\mathrm{T}}$ is the augmented system state, $\bar{\boldsymbol{f}}_i = \left[(\boldsymbol{f}_{\mathrm{ai}} - \dot{\boldsymbol{f}}_{\mathrm{ai}})^{\mathrm{T}}, \boldsymbol{f}_{\mathrm{si}}^{\mathrm{T}}\right]^{\mathrm{T}}$ is the fault. Denote the dimensions of the extended state by $\bar{n} = n + p + q$, then

$$\bar{\boldsymbol{E}} = \begin{bmatrix} \boldsymbol{I}_n & \boldsymbol{0} & \boldsymbol{0} \\ \boldsymbol{0} & \boldsymbol{I}_p & \boldsymbol{0} \\ \boldsymbol{0} & \boldsymbol{0} & \boldsymbol{0}_{q\times q} \end{bmatrix},$$

$$\bar{\boldsymbol{A}} = \begin{bmatrix} \boldsymbol{A} & \boldsymbol{F}_a & \boldsymbol{0} \\ \boldsymbol{0} & \boldsymbol{I}_p & \boldsymbol{0} \\ \boldsymbol{0} & \boldsymbol{0} & \boldsymbol{I}_q \end{bmatrix},$$

$$\bar{B}=\begin{bmatrix} B \\ 0_{p\times n_u} \\ 0_{q\times n_u}\end{bmatrix},$$

$$\bar{F}=\begin{bmatrix} 0_{n\times p} & 0_{n\times q} \\ -I_p & 0 \\ 0 & -I_q\end{bmatrix},$$

$$\bar{C}=\begin{bmatrix} C^{\mathrm{T}} \\ 0_{m\times p}^{\mathrm{T}} \\ F_s^{\mathrm{T}}\end{bmatrix}^{\mathrm{T}}.$$

Remark 2 By extending the actuator and sensor faults to the system state, the sensor faults f_{si} are eliminated from the output equation and replaced by the measurement of the augmented system state $\bar{x}$. Therefore, the fault estimation can be extracted from the system state estimation $\hat{\bar{x}}$ if an observer is designed appropriately for the augmented system (2).

3.1 Distributed observer design

Since $\bar{f}_i(t)$ is unknown and causes an impact on the observation stability, it is preferred to design an observer which is insensitive to the unknown input. Therefore, the following sliding mode-based distributed unknown input observer is proposed.

$$\begin{cases}\bar{S}\dot{\hat{z}}_i=\bar{A}\hat{z}_i+\bar{B}u_i+\bar{K}(y_i-Du_i)+L_su_{\mathrm{si}}+L_pu_{\mathrm{pi}}\\ \hat{\bar{x}}_i=\hat{z}_i+\bar{S}^{-1}L_D(y_i-Du_i)\\ \hat{y}_i=\bar{C}\hat{\bar{x}}_i+Du_i\end{cases}\tag{3}$$

where $\bar{S}=\mathbf{R}^{\bar{n}\times\bar{n}}$ is a non-singular matrix. $u_{\mathrm{si}}\in\mathbf{R}^{p+q}$ and $u_{\mathrm{pi}}\in\mathbf{R}^{m}$ are sliding mode feedback term and distributed feedback term, respectively. $L_s\in\mathbf{R}^{\bar{n}\times(p+q)}$ and $L_p\in\mathbf{R}^{\bar{n}\times m}$ are sliding mode feedback gain matrix and distributed feedback gain matrix, respectively. $\bar{K}\in\mathbf{R}^{\bar{n}\times m}$ and $L_D\in\mathbf{R}^{\bar{n}\times m}$ will be determined later.

Denote the state estimation error as

$$e_i=\hat{\bar{x}}_i-\bar{x}_i.\tag{4}$$

Then, the sliding mode feedback term u_{si} is designed as follows:

$$\begin{cases}s_i=\bar{F}^{\mathrm{T}}\bar{S}^{-\mathrm{T}}\bar{P}e_i\\ u_{\mathrm{si}}=-(\hat{r}_a+\hat{r}_{a\delta}+\hat{r}_s+\varepsilon)\mathrm{sign}(s_i)\end{cases}\tag{5}$$

where $s_i\in\mathbf{R}^{p+q}$ is the sliding mode surface, $P\in\mathbf{R}^{\bar{n}\times\bar{n}}$ is a symmetric positive definite matrix which will be determined later. $\varepsilon>0$ is a parameter designed to guarantee the convergence. $\hat{r}_a$, $\hat{r}_{a\delta}$, and $\hat{r}_s$ are the estimation of r_a, $r_{a\delta}$, and r_s, respectively.

Let $e_{r_a}=\hat{r}_a-r_a$, $e_{r_{a\delta}}=\hat{r}_{a\delta}-r_{a\delta}$, $e_{r_s}=\hat{r}_s-r_s$, and $\varrho\triangleq e_{r_a}+e_{r_{a\delta}}+e_{r_s}+r_a+r_{a\delta}+r_s$, then the sliding mode feedback term can be rewritten as

$$u_{\mathrm{si}}=-(\varrho+\varepsilon)\mathrm{sign}(s_i).\tag{6}$$

The distributed feedback term u_{pi} is designed as follows:

$$u_{\mathrm{pi}}=-\sum_{j=1}^{l}a_{ij}[(\hat{y}_i-y_i)-(\hat{y}_j-y_j)]=$$
$$-\sum_{j=1}^{l}a_{ij}\bar{C}(e_i-e_j).\tag{7}$$

3.2 Error dynamics

The distributed unknown input observer (3), the sliding mode feedback item (5), and the distributed feedback item (7) are designed above. However, some of the parametric matrices used above cannot be determined until the estimation error dynamics reveal its structure step-by-step in the derivation. In this subsection, the main objective is to derive the observation error equation and determine the observer parametric matrices.

In the light of (3), we have

$$\bar{A}\hat{z}_i=\bar{A}\hat{\bar{x}}_i-\bar{A}\bar{S}^{-1}L_D(y_i-Du_i).\tag{8}$$

Taking the time derivative of both sides yields

$$\bar{S}\dot{\hat{\bar{x}}}_i=\bar{S}\left[\dot{\hat{z}}_i+\bar{S}^{-1}L_D(\dot{y}_i-D\dot{u}_i)\right]=$$
$$\bar{A}\hat{z}_i+\bar{B}u_i+\bar{K}(y_i-Du_i)+L_su_{\mathrm{si}}+$$
$$L_pu_{\mathrm{pi}}+L_D(\dot{y}_i-D\dot{u}_i)=$$
$$\bar{A}\hat{\bar{x}}_i-\bar{A}\bar{S}^{-1}L_D(y_i-Du_i)+\bar{K}(y_i-Du_i)+$$
$$\bar{B}u_i+L_su_{\mathrm{si}}+L_pu_{\mathrm{pi}}+L_D\bar{C}\dot{\bar{x}}_i.\tag{9}$$

To eliminate the term y_i-Du_i in (9), $\bar{K}$ is given as follows:

$$\bar{K}\triangleq\bar{A}\bar{S}^{-1}L_D.\tag{10}$$

Substituting (10) into (9) yields

$$\bar{S}\dot{\hat{\bar{x}}}_i=\bar{A}\hat{\bar{x}}_i+\bar{B}u_i+L_su_{\mathrm{si}}+L_pu_{\mathrm{pi}}+L_D\bar{C}\dot{\bar{x}}_i.\tag{11}$$

Comparing (2) and (11), select an appropriate L_D such that

$$\bar{S}\triangleq\bar{E}+L_D\bar{C}\tag{12}$$

which is invertible.

Remark 3 Recalling Assumption 3, one has $\mathrm{rank}(\bar{C})\geqslant q$. Further there exist two matrices $T_L\in\mathbf{R}^{\bar{n}\times m}$ and $T_R\in\mathbf{R}^{m\times\bar{n}}$ satisfying $T_LT_R=\mathrm{diag}(I_m,0_{\bar{n}-m})$ such that $\bar{C}T_R=[\bar{C}_1\ \bar{C}_2]$ where $\mathrm{rank}(C_2)=q$. $L_D=T_L\left[0_{(n-q)\times n}^{\mathrm{T}}\quad \mu((\bar{C}_2^{\mathrm{T}}\bar{C}_2)^{-1}\bar{C}_2^{\mathrm{T}})^{\mathrm{T}}\right]^{\mathrm{T}}$ where $\mu>0$ can be selected such that $\bar{S}$ in (12) which is invertible.

By multiplying $\dot{\bar{x}}_i$ to the both sides of (12), and taking (2) into the result, one has

$$\bar{S}\dot{\bar{x}}_i=\bar{E}\dot{\bar{x}}_i+L_D\bar{C}\dot{\bar{x}}_i=$$
$$\bar{A}\bar{x}_i+\bar{B}u_i+\bar{F}\bar{f}_i+L_D\bar{C}\dot{\bar{x}}_i.\tag{13}$$

According to (4), subtracting (13) from (11) gives the error dynamics equation

$$\dot{\boldsymbol{e}}_i = \bar{\boldsymbol{S}}^{-1}(\bar{\boldsymbol{S}}\dot{\hat{\bar{\boldsymbol{x}}}}_i - \bar{\boldsymbol{S}}\dot{\bar{\boldsymbol{x}}}_i) =$$
$$\bar{\boldsymbol{S}}^{-1}\left[\bar{\boldsymbol{A}}\hat{\bar{\boldsymbol{x}}}_i + \bar{\boldsymbol{B}}\boldsymbol{u}_i + \boldsymbol{L}_s\boldsymbol{u}_{\text{si}} + \boldsymbol{L}_p\boldsymbol{u}_{\text{pi}} + \boldsymbol{L}_D\bar{\boldsymbol{C}}\dot{\hat{\bar{\boldsymbol{x}}}}_i\right] -$$
$$\bar{\boldsymbol{S}}^{-1}\left[\bar{\boldsymbol{A}}\bar{\boldsymbol{x}}_i + \bar{\boldsymbol{B}}\boldsymbol{u}_i + \bar{\boldsymbol{F}}\bar{\boldsymbol{f}}_i + \boldsymbol{L}_D\bar{\boldsymbol{C}}\dot{\bar{\boldsymbol{x}}}_i\right] =$$
$$\bar{\boldsymbol{S}}^{-1}\left[\bar{\boldsymbol{A}}\boldsymbol{e}_i - \bar{\boldsymbol{F}}\bar{\boldsymbol{f}}_i + \boldsymbol{L}_s\boldsymbol{u}_{\text{si}} + \boldsymbol{L}_p\boldsymbol{u}_{\text{pi}}\right]. \quad (14)$$

Denote $\boldsymbol{e} = [\boldsymbol{e}_1^{\mathrm{T}}, \boldsymbol{e}_2^{\mathrm{T}}, \cdots, \boldsymbol{e}_l^{\mathrm{T}}]^{\mathrm{T}}$ as the estimation error of the overall MAS. Let $\bar{\boldsymbol{f}} = \left[\bar{\boldsymbol{f}}_1^{\mathrm{T}}, \bar{\boldsymbol{f}}_2^{\mathrm{T}}, \cdots, \bar{\boldsymbol{f}}_l^{\mathrm{T}}\right]^{\mathrm{T}}$, $\boldsymbol{s} = [\boldsymbol{s}_1^{\mathrm{T}}, \boldsymbol{s}_2^{\mathrm{T}}, \cdots, \boldsymbol{s}_l^{\mathrm{T}}]^{\mathrm{T}}$, $\boldsymbol{u}_s = [\boldsymbol{u}_{s1}^{\mathrm{T}}, \boldsymbol{u}_{s2}^{\mathrm{T}}, \cdots, \boldsymbol{u}_{sl}^{\mathrm{T}}]^{\mathrm{T}}$, $\boldsymbol{u}_p = \left[\boldsymbol{u}_{p1}^{\mathrm{T}}, \boldsymbol{u}_{p2}^{\mathrm{T}}, \cdots, \boldsymbol{u}_{pl}^{\mathrm{T}}\right]^{\mathrm{T}}$. The error dynamics of the overall system is formulated as follows:

$$\dot{\boldsymbol{e}} = \boldsymbol{I}_l \otimes \bar{\boldsymbol{S}}^{-1}(\bar{\boldsymbol{A}}e - \bar{\boldsymbol{F}}\bar{\boldsymbol{f}} + \boldsymbol{L}_s\boldsymbol{u}_s) + \mathcal{L} \otimes \bar{S}^{-1}\boldsymbol{L}_p\boldsymbol{u}_p. \quad (15)$$

This subsection sheds light on the precise expression of the observer. However, the parameters have not yet been determined.

3.3 Stability analysis

In this subsection, we will analyze the stability of the estimation error dynamics (15), and determine the parameters and the adaptive law for the observer (3).

Theorem 1 Take $\boldsymbol{L}_p = \eta\bar{\boldsymbol{S}}\bar{\boldsymbol{C}}^{\mathrm{T}}$ and $\boldsymbol{L}_s = \bar{\boldsymbol{F}}$, where $\eta \in \mathbf{R}^+$ is an adjustable gain coefficient. The adaptive law of the sliding mode feedback term (5) is designed as

$$\begin{cases} \dot{\hat{r}}_a = \alpha\|\boldsymbol{s}_i\| \\ \dot{\hat{r}}_{a\delta} = \beta\|\boldsymbol{s}_i\| \\ \dot{\hat{r}}_s = \gamma\|\boldsymbol{s}_i\| \end{cases} \quad (16)$$

where $\alpha, \beta, \gamma \in \mathbf{R}^+$ are adjustable parameters. There exists a symmetric positive definite matrix $\boldsymbol{P}$, and a matrix $\bar{\boldsymbol{H}} \in \mathbf{R}^{(p+q)\times m}$ that hold the following inequation and equation:

$$\boldsymbol{P}\bar{\boldsymbol{S}}^{-1}\bar{\boldsymbol{A}} + \bar{\boldsymbol{A}}^{\mathrm{T}}\bar{\boldsymbol{S}}^{-\mathrm{T}}\boldsymbol{P} \le \boldsymbol{0}, \quad (17)$$

$$\bar{\boldsymbol{F}}^{\mathrm{T}}\bar{\boldsymbol{S}}^{-\mathrm{T}}\boldsymbol{P} = \bar{\boldsymbol{H}}\bar{\boldsymbol{C}}, \quad (18)$$

then the estimation error $\boldsymbol{e}$ of the distributed observer (3) converges to 0.

Proof To analyze the stability of the estimation error (15), we choose the Lyapunov function candidate as follows:

$$V(t) = \boldsymbol{e}^{\mathrm{T}}(\boldsymbol{I}_l \otimes \bar{\boldsymbol{P}})\boldsymbol{e} + \frac{1}{\alpha}e_{r_a}^2 + \frac{1}{\beta}e_{r_{a\delta}}^2 + \frac{1}{\gamma}e_{r_s}^2. \quad (19)$$

Taking time derivative of $V(t)$ yields

$$\dot{V}(t) = 2\boldsymbol{e}^{\mathrm{T}}(\boldsymbol{I}_l \otimes \boldsymbol{P}\bar{\boldsymbol{S}}^{-1})\left[\boldsymbol{I}_l \otimes (\bar{\boldsymbol{A}}\boldsymbol{e} - \bar{\boldsymbol{F}}\bar{\boldsymbol{f}} - \boldsymbol{L}_s\boldsymbol{u}_s)\right] -$$
$$2\boldsymbol{e}^{\mathrm{T}}(\boldsymbol{I}_l \otimes \boldsymbol{P}\bar{\boldsymbol{S}}^{-1})\left[\mathcal{L} \otimes \boldsymbol{L}_p\boldsymbol{u}_p\right] +$$
$$\frac{2}{\alpha}e_{r_a}\dot{e}_{r_a} + \frac{2}{\beta}e_{r_{a\delta}}\dot{e}_{r_{a\delta}} + \frac{2}{\gamma}e_{r_s}\dot{e}_{r_s}. \quad (20)$$

Recalling (5) and Theorem 1, one has

$$-\boldsymbol{e}_i^{\mathrm{T}}\boldsymbol{P}\bar{\boldsymbol{S}}^{-1}\boldsymbol{L}_s\boldsymbol{u}_s = -(\varrho + \varepsilon)\boldsymbol{e}_i^{\mathrm{T}}\boldsymbol{P}\bar{\boldsymbol{S}}^{-1}\bar{\boldsymbol{F}}\operatorname{sign}(\boldsymbol{s}_i) =$$
$$-(\varrho + \varepsilon)\|\boldsymbol{s}_i\|. \quad (21)$$

Furthermore, we have

$$\boldsymbol{e}_i^{\mathrm{T}}\boldsymbol{P}\bar{\boldsymbol{S}}^{-1}(-\bar{\boldsymbol{F}} \cdot \bar{\boldsymbol{f}}_i + \boldsymbol{L}_s\boldsymbol{u}_{\text{si}}) =$$
$$-\boldsymbol{e}_i^{\mathrm{T}}\boldsymbol{P}\bar{\boldsymbol{S}}^{-1}\bar{\boldsymbol{F}} \cdot \bar{\boldsymbol{f}}_i - (\varrho + \varepsilon)\|\boldsymbol{s}_i\| \leqslant$$
$$\|\boldsymbol{e}_i^{\mathrm{T}}\boldsymbol{P}\bar{\boldsymbol{S}}^{-1}\bar{\boldsymbol{F}}\|\|\bar{\boldsymbol{f}}_i\| - (\varrho + \varepsilon)\|\boldsymbol{s}_i\| =$$
$$\|\boldsymbol{s}_i\|\|\bar{\boldsymbol{f}}_i\| - (\varrho + \varepsilon)\|\boldsymbol{s}_i\| \leqslant$$
$$(r_a + r_{a\delta} + r_s)\|\boldsymbol{s}_i\| - (\varrho + \varepsilon)\|\boldsymbol{s}_i\| =$$
$$-(e_{r_a} + e_{r_{a\delta}} + e_{r_s} + \varepsilon)\|\boldsymbol{s}_i\|. \quad (22)$$

Since r_a, $r_{a\delta}$, and r_s are constants, one has $\dot{e}_{r_a} = \dot{\hat{r}}_a, \dot{e}_{r_{a_\delta}} = \dot{\hat{r}}_{a_\delta}$, and $\dot{e}_{r_s} = \dot{\hat{r}}_s$. In the light of the adaptive law (16), we have

$$\boldsymbol{e}_i^{\mathrm{T}}\boldsymbol{P}\bar{\boldsymbol{S}}^{-1}(-\bar{\boldsymbol{F}} \cdot \bar{\boldsymbol{f}}_i + \boldsymbol{L}_s\boldsymbol{u}_{si}) + \frac{1}{\alpha}e_{r_a}\dot{e}_{r_a} +$$
$$\frac{1}{\beta}e_{r_{a\delta}}\dot{e}_{r_{a\delta}} + \frac{1}{\gamma}e_{r_s}\dot{e}_{r_s} = -\varepsilon\|\boldsymbol{s}_i\|. \quad (23)$$

Furthermore, by substituting (23) into the form of the overall system (15), the following result is obtained:

$$2\boldsymbol{e}^{\mathrm{T}}(\boldsymbol{I}_l \otimes \boldsymbol{P}\bar{\boldsymbol{S}}^{-1})\left[-(\boldsymbol{I}_l \otimes \bar{\boldsymbol{F}})\bar{\boldsymbol{f}} - (\boldsymbol{I}_l \otimes \boldsymbol{L}_s)\boldsymbol{u}_s\right] \leqslant$$
$$-2\epsilon\sum_{i=1}^{l}\|\boldsymbol{s}_i\| \leqslant -2\varepsilon\|\boldsymbol{s}\|. \quad (24)$$

Notice that $\boldsymbol{P}$ and $\bar{\boldsymbol{C}}^{\mathrm{T}}\bar{\boldsymbol{C}}$ are symmetric positive matrices, thus we have $\boldsymbol{P}\bar{\boldsymbol{C}}^{\mathrm{T}}\bar{\boldsymbol{C}} = (\boldsymbol{P}\bar{\boldsymbol{C}}^{\mathrm{T}}\bar{\boldsymbol{C}})^{\mathrm{T}}$. Let $\boldsymbol{\Gamma} = \boldsymbol{P}\bar{\boldsymbol{S}}^{-1}\bar{\boldsymbol{A}} + \bar{\boldsymbol{A}}^{\mathrm{T}}\bar{\boldsymbol{S}}^{-\mathrm{T}}\boldsymbol{P}$ and $\boldsymbol{\Xi} = \boldsymbol{P}\bar{\boldsymbol{C}}^{\mathrm{T}}\bar{\boldsymbol{C}} + \bar{\boldsymbol{C}}^{\mathrm{T}}\bar{\boldsymbol{C}}\boldsymbol{P}$. According to Theorem 1 and Lemma 1, the Lyapunov function derivative (20) becomes

$$\dot{V}(t) \leqslant 2\boldsymbol{e}^{\mathrm{T}}\boldsymbol{I}_l \otimes \boldsymbol{P}\bar{\boldsymbol{S}}^{-1}\left[\boldsymbol{I}_l \otimes \bar{\boldsymbol{A}}\boldsymbol{e} - \mathcal{L} \otimes \boldsymbol{L}_p\boldsymbol{u}_p\right] - 2\varepsilon\|\boldsymbol{s}\| =$$
$$\boldsymbol{e}^{\mathrm{T}}(\boldsymbol{I}_l \otimes \boldsymbol{\Gamma})\boldsymbol{e} - 2\varepsilon\|\boldsymbol{s}\| -$$
$$\boldsymbol{e}^{\mathrm{T}}\left[\mathcal{L} \otimes \boldsymbol{P}\bar{\boldsymbol{S}}^{-1}\boldsymbol{L}_p\bar{\boldsymbol{C}} + \mathcal{L}^{\mathrm{T}} \otimes (\bar{\boldsymbol{S}}^{-1}\boldsymbol{L}_p\bar{\boldsymbol{C}})^{\mathrm{T}}\boldsymbol{P}\right]\boldsymbol{e} =$$
$$\boldsymbol{e}^{\mathrm{T}}(\boldsymbol{I}_l \otimes \boldsymbol{\Gamma})\boldsymbol{e} - 2\varepsilon\|\boldsymbol{s}\| -$$
$$\boldsymbol{e}^{\mathrm{T}}\left[\boldsymbol{\eta}(\mathcal{L} + \mathcal{L}^{\mathrm{T}}) \otimes \boldsymbol{\Xi}\right]\boldsymbol{e}. \quad (25)$$

In the light of Lemma 1, the Lyapunov derivative (25) become

$$\dot{V}(t) \leqslant \boldsymbol{e}^{\mathrm{T}}(\boldsymbol{I}_l \otimes \boldsymbol{\Gamma})\boldsymbol{e} - \boldsymbol{\eta}\boldsymbol{e}^{\mathrm{T}}[\Lambda \otimes \boldsymbol{\Xi}]\boldsymbol{e} - 2\varepsilon\|\boldsymbol{s}\|. \quad (26)$$

Since $\boldsymbol{P}\bar{\boldsymbol{C}}^{\mathrm{T}}\bar{\boldsymbol{C}} + \bar{\boldsymbol{C}}^{\mathrm{T}}\bar{\boldsymbol{C}}\boldsymbol{P} \ge \boldsymbol{0}$, according to Theorem 1 there is $\dot{V}(t) \leqslant 0$, thus the estimation error system (15) is asymptotic stable, that is, the observer (3) is able to track the system (2). □

Remark 4 In (18), only when $\bar{\boldsymbol{C}} \in \mathbf{R}^{m\times\bar{n}}$ satisfies $\operatorname{rank}(\bar{\boldsymbol{C}}) \geqslant \bar{n}$, $\bar{\boldsymbol{H}}$ can be calculated by $\bar{\boldsymbol{H}} = \bar{\boldsymbol{F}}^{\mathrm{T}}\bar{\boldsymbol{S}}^{-\mathrm{T}}\boldsymbol{P}\bar{\boldsymbol{C}}^{+}$

where $\bar{\boldsymbol{C}}^{+}$ is the pseudo-inverse of $\bar{\boldsymbol{C}}$. However, it is impossible to find a suitable $\bar{\boldsymbol{H}}$ to make (18) hold when $m<\bar{n}$ or $\operatorname{rank}(\bar{\boldsymbol{C}})<\bar{n}$. Thus we need an alternative solution to find a suitable $\bar{\boldsymbol{H}}$. Equation (18) is equivalent to

$$\operatorname{Trace}\left[(\bar{\boldsymbol{F}}^{\mathrm{T}}\bar{\boldsymbol{S}}^{-\mathrm{T}}\boldsymbol{P}-\bar{\boldsymbol{H}}\bar{\boldsymbol{C}})^{\mathrm{T}}(\bar{\boldsymbol{F}}^{\mathrm{T}}\bar{\boldsymbol{S}}^{-\mathrm{T}}\boldsymbol{P}-\bar{\boldsymbol{H}}\bar{\boldsymbol{C}})\right]=0. \tag{27}$$

The above equation can be approximated by solving the following inequality [36]:

$$(\bar{\boldsymbol{F}}^{\mathrm{T}}\bar{\boldsymbol{S}}^{-\mathrm{T}}\boldsymbol{P}-\bar{\boldsymbol{H}}\bar{\boldsymbol{C}})^{\mathrm{T}}(\bar{\boldsymbol{F}}^{\mathrm{T}}\bar{\boldsymbol{S}}^{-\mathrm{T}}\boldsymbol{P}-\bar{\boldsymbol{H}}\bar{\boldsymbol{C}})<\epsilon\boldsymbol{I}_{n+p+q} \tag{28}$$

where $\epsilon>0$ is small enough. Furthermore, according to Schur complement, (28) can be transformed into the following linear matrix inequality:

$$\begin{bmatrix} -\epsilon\boldsymbol{I}_{\bar{n}} & (\bar{\boldsymbol{F}}^{\mathrm{T}}\bar{\boldsymbol{S}}^{-\mathrm{T}}\boldsymbol{P}-\bar{\boldsymbol{H}}\bar{\boldsymbol{C}})^{\mathrm{T}} \\ * & -\boldsymbol{I}_{p+q} \end{bmatrix}<\boldsymbol{0} \tag{29}$$

where $*$ represents the element that forms a symmetric matrix.

Remark 5 The parameters and matrices of the proposed method are calculated or selected in the following sequence:

Step 1 Select an appropriate $\boldsymbol{L}_D$ that makes the $\bar{\boldsymbol{S}}$ in (12) invertible.

Step 2 Calculate $\bar{\boldsymbol{K}}$ by (10) with $\bar{\boldsymbol{S}}$ from Step 1.

Step 3 Solve matrix inequalities (17) and (19) to obtain $\boldsymbol{P}$ and $\bar{\boldsymbol{H}}$.

Step 4 Select an appropriate $\eta>0$ to tune the tracking performance of the distributed observer.

Step 5 Select appropriate $\alpha, \beta, \gamma>0$ for the adaptive laws (16).

4. Simulations

This section presents a numerical simulation to demonstrate the effectiveness of the proposed fault diagnosis method. Considering a MAS consisting of five agents, the communication topology is shown in Fig. 1.

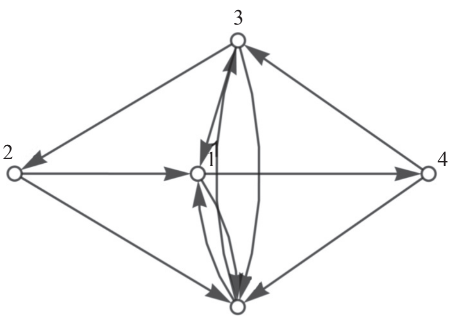

Fig. 1 Connections among agents

The system matrices of each agent are taken as

$$\boldsymbol{A}=\begin{bmatrix} -1 & 1 & 0 \\ 1 & -2 & 1 \\ 0 & 1 & -1 \end{bmatrix},$$

$$\boldsymbol{B}=\begin{bmatrix} 0 \\ 1 \\ 1 \end{bmatrix},$$

$$\boldsymbol{D}=\begin{bmatrix} 1 \\ 2 \\ 2 \end{bmatrix},$$

$$\boldsymbol{C}=\begin{bmatrix} 1 & 2 & -1 \\ 0 & 1 & 0 \\ 1 & 1 & 2 \end{bmatrix},$$

$$\boldsymbol{F}_a=\begin{bmatrix} 1 \\ 1 \\ 1 \end{bmatrix},$$

$$\boldsymbol{F}_s=\begin{bmatrix} 1 \\ -2 \\ 1 \end{bmatrix}.$$

The following commonly used control law is deployed on the MAS [37,38]:

$$\boldsymbol{u}_i(t)=-\boldsymbol{K}_u\sum_{j=1,j\neq i}^{l}a_{ij}(\boldsymbol{y}_i(t)-\boldsymbol{y}_j(t)) \tag{30}$$

where $\boldsymbol{K}_u=-\begin{bmatrix} 7.625 & 6.125 & 0.875 \end{bmatrix}$ is the control gain.

The observer parameters are determined as follows. Let $\boldsymbol{T}_L=\boldsymbol{T}_R^{\mathrm{T}}=[\boldsymbol{I}_m, \boldsymbol{0}_{m\times(\bar{n}-m)}]^{\mathrm{T}}$, then calculate $\boldsymbol{L}_D$ according to Remark 3. $\bar{\boldsymbol{S}}$ and $\bar{\boldsymbol{K}}$ are then calculated by (12) and (10), respectively. $\boldsymbol{P}$ and $\bar{\boldsymbol{H}}$ are calculated according to (17) and (29), respectively. Let $\eta=1$, $\boldsymbol{L}_p$ is then calculated according to Theorem 1. $\boldsymbol{P}$ and $\bar{\boldsymbol{H}}$ are given as

$$\boldsymbol{P}=10^{-2}\times\begin{bmatrix} 5.67 & -7.97 & 2.18 & -0.26 & 2.04 \\ -7.97 & 11.45 & -3.4 & 0.16 & -1.31 \\ 2.18 & -3.4 & 1.3 & 0.16 & -1.43 \\ -0.26 & 0.16 & 0.16 & 0.21 & -1.05 \\ 2.04 & -1.31 & -1.43 & -1.05 & 12.29 \end{bmatrix},$$

$$\bar{\boldsymbol{H}}=10^{-3}\times\begin{bmatrix} 1.6 & -4.5 & 0.1 \\ 0.7 & 0.4 & -0.3 \end{bmatrix}.$$

For the adaptive laws, $\alpha=20$, $\beta=30$, and $\gamma=50$ are taken, the initial values are $\hat{r}_a(0)=\hat{r}_{a\delta}(0)=\hat{r}_s(0)=0$.

The initial states x_{1-5} of the agents are set as random values between -10 and 10. $\hat{z}_{1-5}(0)=[0,0,0,0,0]^{\mathrm{T}}$ is taken for all observers. There are four scenarios simulated: fault-free, actuator fault, sensor fault, and concurrent fault.

4.1 Scenario: fault-free

Firstly, a fault-free scenario is simulated to illustrate the estimation effect of the proposed method under the fault-free situation.

The results are shown as Figs. 2–5. In the following simulation results, the actual value of the states and faults are illustrated in the colored solid line, while the estimated value is in the dashed line with the same color. As can be seen from Fig. 2, the estimation errors converge to finetune stage in two seconds. Fig. 3 shows that $\hat{x}_{1-5}$ converges in 3 s and then reaches x_{1-5} under the driving of the distributed feedback term. Fig. 4 and Fig. 5 show that the actuator and sensor faults estimation converge to the actual value in $t < 3$ s.

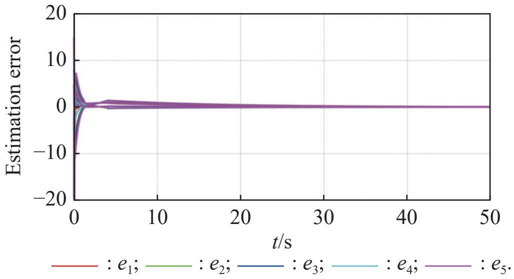

Fig. 2 Fault-free scenario: estimation error e_{1-5}

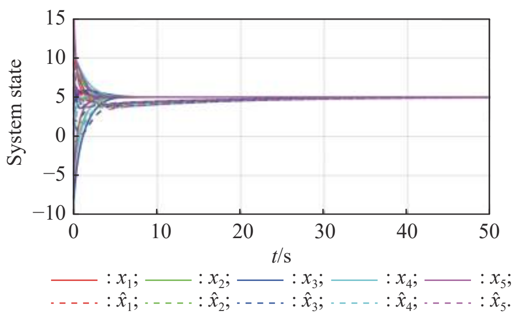

Fig. 3 Fault-free scenario: x and $\hat{x}$

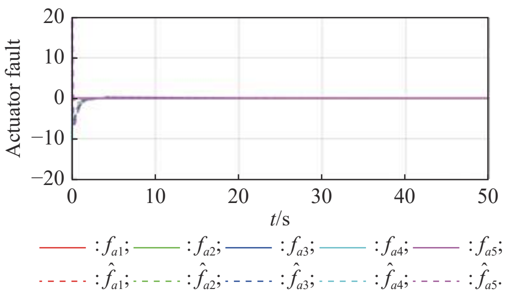

Fig. 4 Fault-free scenario: f_a and $\hat{f}_a$

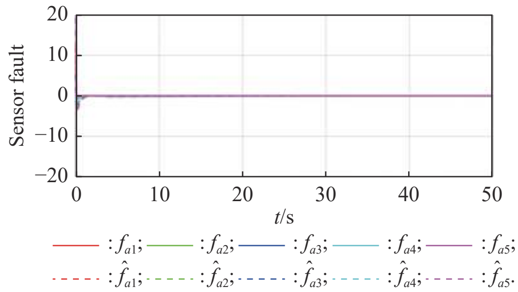

Fig. 5 Fault-free scenario: f_s and $\hat{f}_s$

4.2 Scenario: actuator fault

In this scenario, agent 1 is injected by the actuator fault (31). The results are shown in Figs. 6–9. Fig. 6 shows that the error e_1 spikes at $t = 15$ s and then converges to 0 in less than 1 s. Fig. 8 reveals the reason of the spike is that $f_{a1}(15) \neq 0$. Fig. 9 shows that affected by the actuator fault (31), the sensor fault estimation also spikes at $t = 15$ s. Comparing with fault-free scenarios, although the actuator fault causes the system unstability, the estimation $\hat{x}_{1-5}$ still track the system state x_{1-5} well. As shown in Fig. 6, due to the adaptive law, the estimation error bound $\|e_{1-5}\|$ becomes smaller over time which means the observer achieves better estimation over time.

$$f_{\mathrm{ai}}(t) = \begin{cases} 0, & 0\ \mathrm{s} \leqslant t < 15\ \mathrm{s} \\ 20\sin(0.5t), & t \geqslant 15\ \mathrm{s} \end{cases} \tag{31}$$

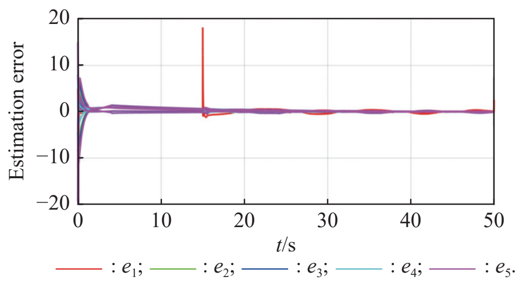

Fig. 6 Actuator fault scenario: estimation error: e_{1-5}

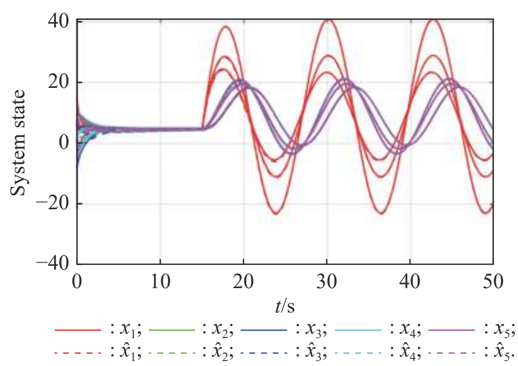

Fig. 7 Actuator fault scenario: x and $\hat{x}$

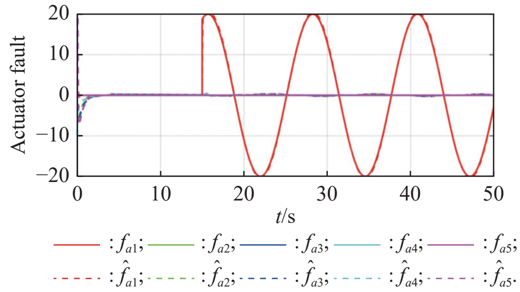

Fig. 8 Actuator fault scenario: f_a and $\hat{f}_a$

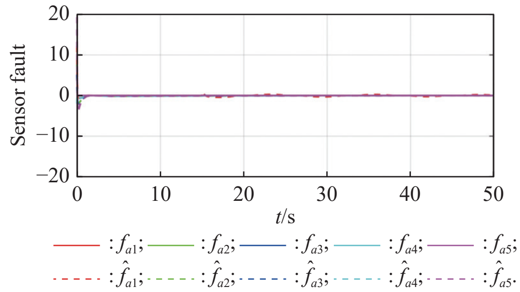

Fig. 9 Actuator fault scenario: f_s and $\hat{f}_s$

4.3 Scenario: sensor fault

To demonstrate the sensor fault effectiveness of the proposed method, agent 2 is injected by the sensor fault (32). The results are shown in Figs. 10–13. The sensor fault driving the system state fluctuates in $t \geqslant 10$ s which is estimated timely. Comparing with Figs. 6–9, the sensor fault does not cause noticeable influence on estimation error $e_{1\text{–}5}$ or actuator fault estimation $\hat{f}_{ai}$.

$$f_{si}(t) = \begin{cases} 0, & 0 \text{ s} \leqslant t < 20 \text{ s} \\ 20\sin(0.5t), & t \geqslant 20 \text{ s} \end{cases} \tag{32}$$

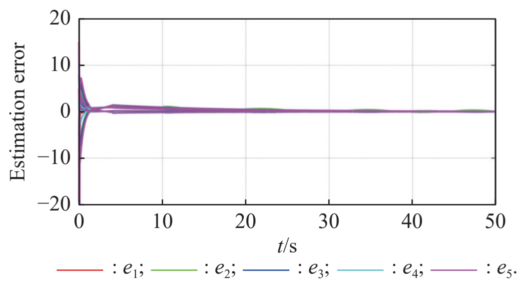

Fig. 10 Sensor fault scenario: estimation error: $e_{1\text{–}5}$

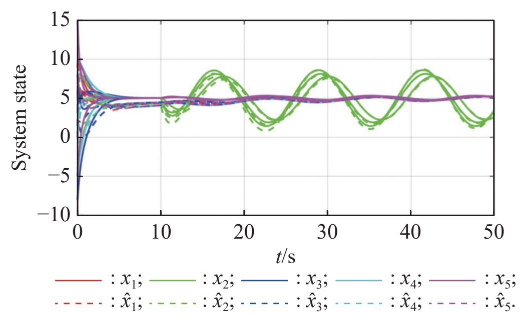

Fig. 11 Sensor fault scenario: x and $\hat{x}$

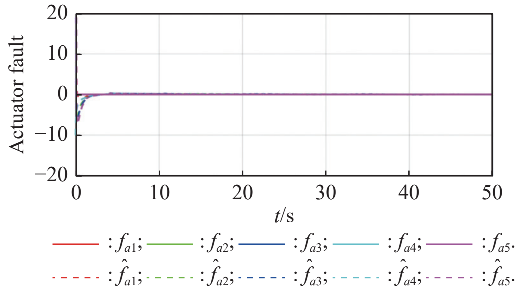

Fig. 12 Sensor fault scenario: f_a and $\hat{f}_a$

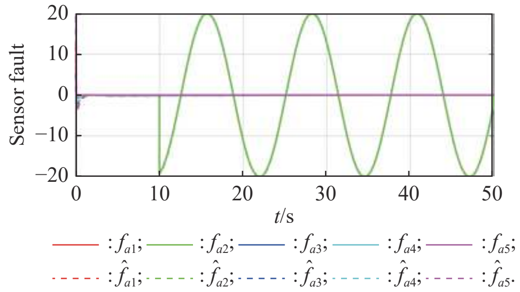

Fig. 13 Sensor fault scenario: f_s and $\hat{f}_s$

4.4 Scenario: concurrent fault

In this simulation, agent 1 and agent 2 are injected by actuator fault (31) and sensor fault (32), respectively. The results are shown as Figs. 14–17. It can be seen from Fig. 14 that the estimation error $e_{1\text{–}5}$ converge to a small region around 0 in 3 s. The similarity between Fig. 14 and Fig. 6 demonstrates the effectiveness of MAS actuator and sensor fault diagnosis.

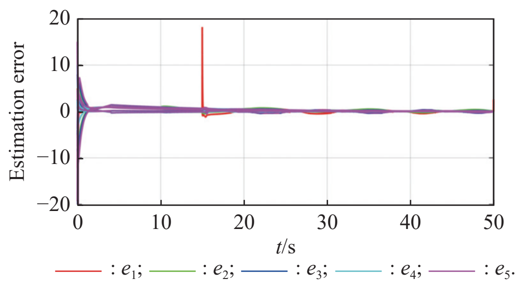

Fig. 14 Concurrent fault scenario: estimation error: $e_{1\text{–}5}$

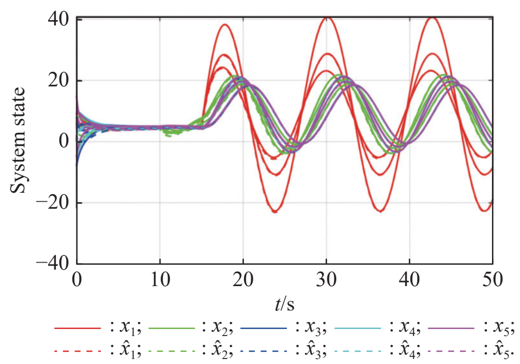

Fig. 15 Concurrent fault scenario: x and $\hat{x}$

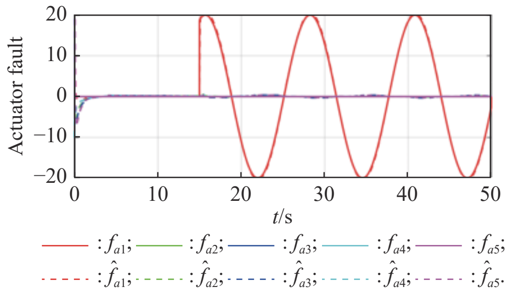

Fig. 16 Concurrent fault scenario: f_a and $\hat{f}_a$

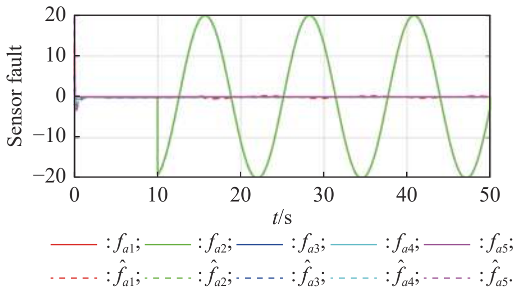

Fig. 17 Concurrent fault scenario: f_s and $\hat{f}_s$

In a conclusion, the proposed method achieves ideal estimation of the MAS states regardless of the actuator fault, sensor fault, or concurrent fault. The actuator fault and sensor fault are also diagnosed effectively in the same time.

5. Conclusions

In this paper, the problem of actuator and sensor fault diagnosis for MAS has been considered. The descriptor system approach has been introduced to eliminate the sensor fault in the measurement function. An adaptive law is adopted to adjust the gains of the sliding mode-based distributed observer and reduce the priori knowledge requirements of the MAS. Numerical simulations demonstrate the effectiveness of the proposed method.

References

[1] JIN X Z, LU S Y, DENG C, et al. Distributed adaptive security consensus control for a class of multi-agent systems under network decay and intermittent attacks. Information Sciences, 2021, 547: 88–102.

[2] YU Z Q, ZHANG Y M, JIANG B. PID-type fault-tolerant prescribed performance control of fixed-wing UAV. Journal of Systems Engineering and Electronics, 2021, 32(5): 1053–1061.

[3] SHAKHATREH H, SAWALMEH A H, AL-FUQAHA A, et al. Unmanned aerial vehicles (UAVs): a survey on civil applications and key research challenges. IEEE Access, 2019, 7: 48572–48634.

[4] WANG T, HUANG P F, DONG G Q. Cooperative persistent surveillance on a road network by multi-UGVs with detection ability. IEEE Trans. on Industrial Electronics, 2021, 69(11): 11468–11478.

[5] HU J Y, BHOWMICK P, JANG I, et al. A decentralized cluster formation containment framework for multirobot systems. IEEE Trans. on Robotics, 2021, 37(6): 1936–1955.

[6] KADA B, KHALID M, SHAIKH M S. Distributed cooperative control of autonomous multi-agent UAV systems using smooth control. Journal of Systems Engineering and Electronics, 2020, 31(6): 1297–1307.

[7] CHENG W L, ZHANG K, JIANG B, et al. Fixed-time fault-tolerant formation control for heterogeneous multi-agent systems with parameter uncertainties and disturbances. IEEE Trans. on Circuits and Systems I: Regular Papers, 2021, 68(5): 2121–2133.

[8] CHENG W L, JIANG B, ZHANG K, et al. Robust finite-time cooperative formation control of UGV-UAV with model uncertainties and actuator faults. Journal of the Franklin Institute, 2021, 358(17): 8811–8837.

[9] YANG P, MA B, DONG Y, et al. Fault-tolerant consensus of leader-following multi-agent systems based on distributed fault estimation observer. International Journal of Control, Automation and Systems, 2018, 16(5): 2354–2362.

[10] XU X L, LI Z T, GAO L X. Distributed adaptive tracking control for multi-agent systems with uncertain dynamics. Nonlinear Dynamics, 2017, 90(4): 2729–2744.

[11] BOEM F, GALLO A J, RAIMONDO D M, et al. Distributed fault-tolerant control of large-scale systems: an active fault diagnosis approach. IEEE Trans. on Control of Network Systems, 2019, 7(1): 288–301.

[12] ZHANG K, JIANG B, CHEN M, et al. Distributed fault estimation and fault-tolerant control of interconnected systems. IEEE Trans. on Cybernetics, 2019, 51(3): 1230–1240.

[13] AMIN A A, HASANA K M. A review of fault tolerant control systems: advancements and applications. Measurement, 2019, 143: 58–68.

[14] LI D L, WANG Y, WANG J X, et al. Recent advances in sensor fault diagnosis: a review. Sensors and Actuators A: Physical, 2020, 309: 111990.

[15] YU Y, ZHAO Y Z, WANG B, et al. Current sensor fault diagnosis and tolerant control for VSI-based induction motor drives. IEEE Trans. on Power Electronics, 2017, 33(5): 4238–4248.

[16] WU Y K, JIANG B, WANG Y L. Incipient winding fault detection and diagnosis for squirrel-cage induction motors equipped on CRH trains. ISA Transactions, 2020, 99: 488–495.

[17] SHAHNAZARI H, MHASKAR P. Distributed fault diagnosis for networked nonlinear uncertain systems. Computers & Chemical Engineering, 2018, 115: 22–33.

[18] LI J, PAN K P, SU Q Y. Sensor fault detection and estimation for switched power electronics systems based on sliding mode observer. Applied Mathematics and Computation, 2019, 353: 282–294.

[19] ZHANG J, LI S, XIANG Z R. Adaptive fuzzy finite-time fault tolerant control for switched nonlinear large-scale systems with actuator and sensor faults. Journal of the Franklin Institute, 2020, 357(16): 11629–11644.

[20] DU D S. Fault detection for discrete-time linear systems based on descriptor observer approach. Applied Mathematics and Computation, 2017, 293: 575–585.

[21] CHEN T R, ZHU Z J, WANG C, et al. Rapid sensor fault diagnosis for a class of nonlinear systems via deterministic learning. IEEE Trans. on Neural Networks and Learning Systems, 2022, 33(12): 7743–7754.

[22] LIU M, SHI P. Sensor fault estimation and tolerant control

for Itô stochastic systems with a descriptor sliding mode approach. Automatica, 2013, 49(5): 1242–1250.

[23] GAO Z W, DING S X. Sensor fault reconstruction and sensor compensation for a class of nonlinear state-space systems via a descriptor system approach. IET Control Theory & Applications, 2007, 1(3): 578–585.

[24] LI X H, AHN C K, LU D K, et al. Robust simultaneous fault estimation and nonfragile output feedback fault-tolerant control for Markovian jump systems. IEEE Trans. on Systems, Man, and Cybernetics, 2018, 49(9): 1769–1776.

[25] WU Y K, JIANG B, LU N Y. A descriptor system approach for estimation of incipient faults with application to high-speed railway traction devices. IEEE Trans. on Systems, Man, and Cybernetics: Systems, 2017, 49(10): 2108–2118.

[26] GOMEZ-PENATE S, VALENCIA-PALOMO G, LOPEZESTRADA F R, et al. Sensor fault diagnosis based on a $\mathcal{H}_\infty$ sliding mode and unknown input observer for Takagi-Sugeno systems with uncertain premise variables. Asian Journal of Control, 2019, 21(1): 339–353.

[27] YIN S, GAO H J, QIU J B, et al. Descriptor reduced-order sliding mode observers design for switched systems with sensor and actuator faults. Automatica, 2017, 76: 282–292.

[28] GAO Z W, WANG H. Descriptor observer approaches for multivariable systems with measurement noises and application in fault detection and diagnosis. Systems & Control Letters, 2006, 55(4): 304–313.

[29] ZHU J W, YANG G H, ZHANG W A. Cooperative fault tolerant tracking control for multiagent systems: an intermediate estimator-based approach. IEEE Trans. on Cybernetics, 2018, 48(10): 2972–2980.

[30] HANG J, LIU X H, GAO X W, et al. Intermediate observer-based robust distributed fault estimation for nonlinear multiagent systems with directed graphs. IEEE Trans. on Industrial Informatics, 2019, 16(12): 7426–7436.

[31] MA H J, XU L. Cooperative fault diagnosis for uncertain nonlinear multiagent systems based on adaptive distributed fuzzy estimators. IEEE Trans. on Cybernetics, 2018, 50(4): 1739–1751.

[32] QIN L G, HE X, YAN R, et al. Distributed sensor fault diagnosis for a formation of multi-vehicle systems. Journal of the Franklin Institute, 2019, 356(2): 791–818.

[33] ZHOU D H, QIN L G, HE X, et al. Distributed sensor fault diagnosis for a formation system with unknown constant time delays. Science China Information Sciences, 2018, 61: 112205.

[34] BALAKRISHNAN R, RANGANATHAN K. A textbook of graph theory. Heidelberg: Springer, 2012.

[35] ZHAN X Z. Matrix theory. Rhode Island: American Mathematical Society, 2013.

[36] NIU Y, LAM J, WANG X, et al. Observer-based sliding mode control for nonlinear state-delayed systems. International Journal of Systems Science, 2004, 35(2): 139–150.

[37] WEI Q L, WANG X, ZHONG X N, et al. Consensus control of leader-following multi-agent systems in directed topology with heterogeneous disturbances. IEEE/CAA Journal of Automatica Sinica, 2021, 8(2): 423–431.

[38] GAO Z R, LI C D, WANG X, et al. Finite-time consensus of linear multi-agent system via distributed event-triggered strategy. Journal of the Franklin Institute, 2018, 355(3): 1338–1350.

Biographies

YE Zhengyu was born in 1995. He received his M.S. degree from Nanjing University of Aeronautics and Astronautics, Nanjing, China, in 2017, where he is currently pursuing his Ph.D. degree in control science and engineering. His research interests include sensor fault diagnosis and fault tolerant control of multi-UAV systems.
E-mail: kasoll076@outlook.com

JIANG Bin was born in 1966. He received his Ph.D. degree in automatic control from Northeastern University, Shenyang, China, in 1995. He has been a post-doctoral fellow or a research fellow in Singapore, France, and USA, and a visiting professor in Canada. He is currently the chair professor of the Cheung Kong Scholar Program, Ministry of Education, and the vice president of the Nanjing University of Aeronautics and Astronautics, Nanjing, China. His research interests include fault diagnosis and fault-tolerant control and their applications.
E-mail: binjiang@nuaa.edu.cn

CHENG Yuehua was born in 1977. She received her Ph.D. degree from Nanjing University of Aeronautics and Astronautics, Nanjing, China, in 2013. She is a professor in Nanjing University of Aeronautics and Astronautics. Her research interests include fault tolerant control and life prediction for satellite attitude control systems.
E-mail: chengyuehua@nuaa.edu.cn

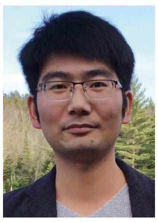

YU Ziquan was born in 1989. He received his Ph.D. degree in control science and engineering from Northwestern Polytechnical University in 2019. From 2017 to 2019, he was a joint Ph.D. student supported by the China Scholarship Council with the Department of Mechanical, Industrial and Aerospace Engineering, Concordia University, Montreal, QC, Canada. He is currently with the College of Automation Engineering, Nanjing University of Aeronautics and Astronautics, Nanjing. His current research interests include fault-tolerant cooperative control of safety-critical systems, and guidance, navigation, and control of unmanned aerial vehicles.
E-mail: yuziquan@nuaa.edu.cn

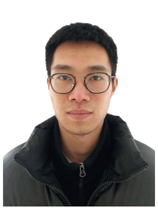

YANG Yang was born in 1998. He received his B.E. degree in automotive engineering in 2020 from Hefei University of Technology and he is pursuing his master's degree in Nanjing University of Aeronautics and Astronautics. His research interests include distributed fault detection and diagnosis of multi-UAVs.
E-mail: youngy@nuaa.edu.cn